Journal of Manufacturing Processes 152 (2025) 1084–1089

Contents lists available at ScienceDirect

Journal of Manufacturing Processes

journal homepage: www.elsevier.com/locate/manpro

# A novel self-generating abrasive jet machining process

Yan Hu [a,b,c], Jianchi Chen [a], Qingwen Dai [a], Wei Huang [a], Jingqiu Wang [a], Xiaolei Wang [a,*]

[a] College of Mechanical and Electrical Engineering, Nanjing University of Aeronautics and Astronautics, Nanjing 210016, China
[b] Anhui Research Center for Generic Technologies in Robot Industry, Anhui Polytechnic University, Wuhu 241000, China
[c] School of Mechanical Engineering, Anhui Polytechnic University, Wuhu 241000, China

ARTICLE INFO

*Keywords:*
Abrasive jet machining
Surface texturing
Soft materials
Particle embedment
Self-generating abrasive jet

ABSTRACT

Abrasive jet is a unique micro-machining technique. Particularly for the purpose of surface texturing, it offers the advantages of broad scalability, high efficiency, and minimal side effects. However, the embedding of hard abrasives into the machined surface, especially for soft materials, causing residue contamination, poses a significant challenge. A novel self-generating abrasive jet machining (SGAJM) is proposed in this study. In this method, compressed air is accelerated through a nozzle, generating a pressure drop and low temperatures. This draws in a saturated salt solution, causing crystalline abrasives to precipitate. Consequently, a multiphase jet is formed, enabling the machining of surface textures while effectively resolving the issue of residual hard abrasives.

## 1. Introduction

The quality of the surface is often of the utmost importance for the correct functioning of the part. Surface texturing, *i.e.*, the microstructures machined on the surface, is showing broad application prospects in improving tribological performance of mechanical components [1,2].

Recent advances in abrasive jet machining (AJM) technology, including abrasive air jet, abrasive slurry jet, multiphase jet and abrasive water jet have shown their extensive applicability in machining process [3–5]. For surface texturing, these AJM technologies offer the benefits such as negligible thermal influence, minimal cutting forces, and environmental friendliness. Especially, according to their processing principles, they have the characteristics of relatively low cost and high efficiency. The processing scale can cover the range from millimeters to micrometers and nanometers. They are capable of fabricating millimeter scale features such as grooves and polishing the surface to mirror level, making them an important supplement to other precision machining technologies.

As a processing tool, AJM can remove almost any material, including rock, metal, ceramics, composites, and biological tissue. In jet machining, the mechanism of surface material removal involves two aspects: micro-cutting caused by the tangential sliding of abrasive particles, and localized brittle fracture of the surface caused by normal impact. Hence, the size of abrasive particles is generally determined by the scale and precision of the processing target, as well as the nozzle size; For the shape of abrasives, angular and sharp abrasive grains offer high processing efficiency, while near-spherical particles provide good flowability in the transportation pipe and yield lower surface roughness. Material-wise, hard substances like silicon carbide (Mohs 9.5), alumina (Mohs 9), and synthetic diamond (Mohs 10) are commonly selected considering the target material (stainless steel and aluminum have Mohs hardness values of 5 and 3, respectively) and cost.

Clearly, one hazard of using hard abrasives is that during high-speed jetting, these hard particles can easily become embedded into the processed surface [6]. For frictional system, this can lead to undesirable consequences during subsequent friction processes, compromising surface integrity. This phenomenon is particularly significant for soft materials. For instance, mechanical seals, besides using ceramics and metals, sometimes employ PTFE (polytetrafluoroethylene) composites in specific applications. They may also require surface texturing on the contact interfaces to further enhance their tribological performance. When AJM is used, hard particles readily embed into the PTFE surface. During seal operation, these embedded abrasives may cause unwanted abrasive wear. Furthermore, studies indicate that these residual particles may act as stress concentration points and crack initiators, leading to reduced surface fatigue life [7].

Many efforts have been conducted to solve the problem of hard

* Corresponding author.
*E-mail address:* wxl@nuaa.edu.cn (X. Wang).

https://doi.org/10.1016/j.jmapro.2025.08.072
Received 10 June 2025; Received in revised form 8 August 2025; Accepted 25 August 2025
Available online 30 August 2025

abrasive residue. The approaches include using the post-cleaning process such as ultrasonic cleaning/plain water jet cleaning/shot peening [7], and optimizing the process by using inclined abrasive jets or cryogenically assisted abrasive jet [8].

On the other hand, researchers are trying to find abrasives that are friendly to the machining surface and can be effectively removed. Zhao et al. suggested that compared to hard abrasives, soft plastic abrasives appear more suitable for specific applications, such as components like marine pumps made of carbon fiber composites [9]. To avoid the surface damage like scratches and pitting caused hard abrasives, Chai et al. used biodegradable walnut shells as abrasives in an abrasive water jet for paint removal [10]. Zhu et al. employed amino thermosetting plastic abrasives in an air jet for machining aluminum alloy [11]. At the International Burring Conference of 2009, Uhlmann [12] and Karpuschewski [13] respectively proposed the $CO_2$ dry snow jet and the ice particle jet. By preparing $CO_2$ dry snow or ice particles of a specific size in advance and using gas propulsion to form a jet, they achieved burr removal from workpieces. These two abrasives sublimate/melt at room temperature, eliminating the problem of hard particle residue. In 2023, Guo et al., aiming to solve the issue of abrasive biocompatibility during osteotomy, selected three types of crystals—sodium chloride, sucrose, and xylitol—as abrasives [14]. They used an ultra-high-speed water jet to entrain the abrasives, mixing and accelerating them in a mixing chamber to form a solid-liquid two-phase crystalline jet for eroding and cutting bone samples.

It is no doubt that the $CO_2$ dry snow jet and ice particle jet are highly innovative ideas. However, at atmospheric pressure, $CO_2$ requires temperatures below −80 °C to form solid dry ice. Furthermore, dry ice has a hardness of only 1.5 Mohs, equivalent to gypsum, and $CO_2$ dry snow is even softer [12]. Consequently, this jetting method is suitable for burr removal on plastic parts. Ice particles made from frozen water face the same issue; ice at 0 °C also has a hardness around 1.5 Mohs. Only when temperatures drop below −40 °C can they exceed 4 Mohs [13]. Another problem with these jets is that maintaining ice particles without agglomeration under freezing conditions requires a complex system. Preventing clogging during transport remains a significant challenge.

Therefore, a self-generating abrasive jet machining (SGAJM) technology is proposed in this paper. A distinctive feature of SGAJM technology lies in its utilization of the aerodynamic cooling effect generated by pressurized air which passes through the nozzle, thereby triggering crystallization in the introduced saturated solution. Unlike traditional ice jets, SGAJM enables simultaneous abrasive preparation and jet formation at the nozzle. Its continuous, rapid, and stable in-nozzle production of crystal abrasive constitutes a key advantage. In this paper, the working principle of SGAJM was clarified. And then, the machining ability of SGAJM on soft materials was investigated, as well as the material removal mechanism.

## 2. Working principle of SGAJM

In all previous abrasive jet methods, solid particles needed to be prepared in advance and then introduced into the jet.

Fig. 1 shows the working principle of the SGAJM process and its schematic diagram for workpiece processing. High-speed airflow is generated when compressed air passes through the airflow outlet inside the nozzle. According to Bernoulli equation for compressible flow of an ideal gas [15],

$$\frac{1}{2}v^2 + gz + \left(\frac{\gamma}{\gamma-1}\right)\frac{p}{\rho} = C \tag{1}$$

where $p$, $v$ present the pressure and flow speed of the fluid, $\rho$ is the density of the fluid, $g$ is the gravitational acceleration, z is the elevation of the point above a reference plane, $\gamma$ is the ration of the specific heats of the fluid, and C is a constant. As the gas flows from one section of a pipe to a smaller section, by Venturi effect, it speeds up, resulting in pressure reduction. The faster the gas flow, the lower the pressure, creating a pressure drop in the nozzle's mixing chamber. Due to this low pressure, a saturated crystal solution with controlled temperature is sucked in from the liquid inlet and mixes with the air.

If air is considered to be an ideal gas, its behavior can be described based on the general law of state [16],

$$p \cdot v_s = R_i \cdot T \tag{2}$$

where $v_s$ presents the specific volume of the gas, $R_i$ is the individual gas constant, and $T$ is the absolute temperature of the gas. This equation shows the relationship between pressure and temperature. The velocity of an air jet exiting a pressurized air reservoir through a small opening can be expressed as the enthalpy difference ($\Delta h_A$) between vessel and environment as

$$v_A = \sqrt{2 \bullet \Delta h_A} \tag{3}$$

Because of the air expansion, the temperature drop of the air at the airflow outlet can be derived as

$$T_d = T_N - T_E = \frac{v_A^2}{2 \bullet c_P} \tag{4}$$

where $T_N$, $T_E$ represent the temperatures of air at the entry and exit, respectively, $c_P$ is the isobaric heat capacity of air [16]. It means the faster the airflow speed, the greater the decrease in temperature.

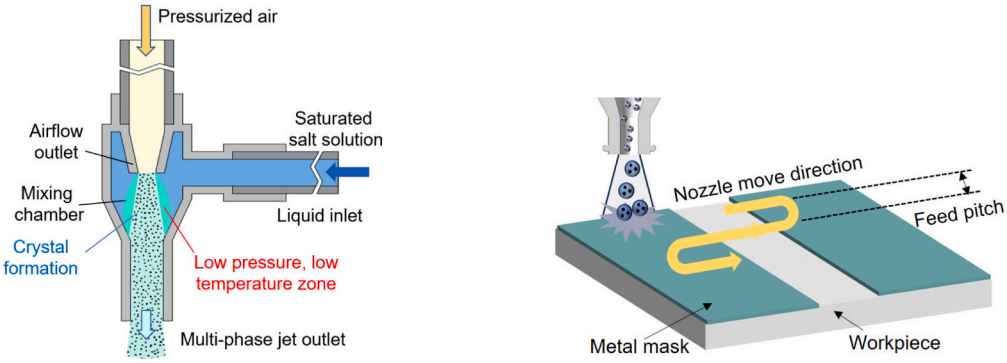


(a) Principle of self-generating abrasive jet (b) Surface texturing process

**Fig. 1.** Schematic diagram of self-generating abrasive jet and its machining process.
(a) Principle of self-generating abrasive jet.
(b) Surface texturing process.

Consequently, the saturated solution mixed with the gas rapidly cools, resulting in crystals to precipitate. The precipitated crystals, entrained by both air and liquid, form a multiphase jet that impacts the workpiece surface for machining.

In order to obtain a specific pattern of surface texture, a metal mask is placed on the workpiece to protect undesired machining area, the nozzle will move by a S-type path to cover the opening area of the mask. The feed pitch of nozzle movement is set smaller than the jet footprint to make sure the workpiece evenly fabricated.

Compared to conventional abrasive air jets, this solution offers several fundamental advantages as follows.

- The problem of abrasive residue is solved by simple rinsing with water because highly soluble crystal is used.
- Compared to $CO_2$ dry snow or ice particle jets, this system is simpler. It eliminates the need for complex cryogenic abrasive preparation and delivery systems. Furthermore, salt crystals formed at room temperature have a higher hardness than $CO_2$ dry snow and ice particles, resulting in higher machining efficiency.
- Abrasive settling and clogging will not occur because only liquid solutions are transported through the suction pipe.
- It retains the benefits of abrasive air jets, namely using a standard low-pressure air source (<1 MPa) to achieve high flow velocities (estimated >100 m/s). This enhances machining efficiency, ensures safety, and reduces costs.
- The machining jet contains solid, liquid, and gas phases, making it a multiphase jet. The previous research has shown that multiphase jets reduce the divergence of air jets and improve focus [17].
- The presence of water helps reducing the suspension of abrasive ejecta in the air, and the solution is easily recovered and reused. Additionally, water provides cooling and lubrication effects, offering the potential to improve the quality of the machined surface. Low-toxicity salts can be selected as abrasives; for example, $NaNO_3$ is a fertilizer with minimal environmental impact.

## 3. Abrasive selection

In the SGAJM process, abrasives are generated inside the nozzle by crystallization and precipitation due to the decrease in temperature. The selection of appropriate crystal to make saturated solution is therefore critical, as it directly influences the precipitation of crystals and their machining performance. The solubility of the dissolved substance in water should decrease with dropping temperature, with a larger change being more desirable. Fig. 2 shows the solubility curves of four selected salts as a function of temperature. Although NaCl is the most common and low toxicity salt, its solubility shows little change with increasing temperature; thus, the low-temperature environment within the nozzle cannot induce NaCl precipitation. For this reason, $NaNO_3$, $NaH_2PO_4$, and $CaCl_2$ were selected for the experiments, among which $NaH_2PO_4$ has the largest solubility/temperature slope, and the average slopes of $NaNO_3$ and $CaCl_2$ were roughly equivalent.

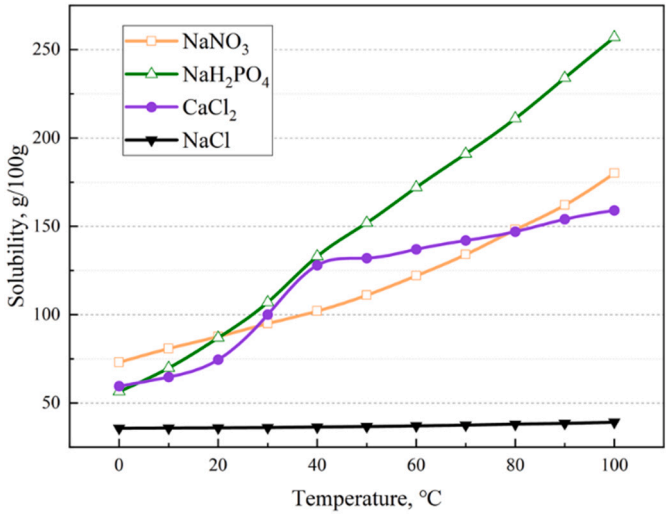


**Fig. 2.** The solubility curves of four selected salts as a function of temperature.

## 4. Machining ability of the salt solutions

The nozzle of the SGAJM jet is the key component responsible for creating low pressure and low temperatures in mixing chamber, so that to generate crystallized abrasives. The shape and size of the nozzle's airflow outlet, mixing chamber, liquid suction inlet, and jet outlet can all potentially influence the formation of crystallized abrasives. To rapidly validate the effectiveness of SGAJM jet processing, a preliminary CFD simulation was conducted to roughly optimize the SGAJM jet nozzle, ensuring low pressure formation within the mixing chamber.

Subsequently, saturated solutions of each of the aforementioned three salts were prepared and maintained at temperatures of 30 °C, 40 °C, and 50 °C, based on their respective solubilities. Using the processing method illustrated in Fig. 1, machining experiments were performed on PTFE material with the same operational conditions. Specific processing parameters and the information of the mask are detailed in Table 1.

Fig. 3 displays the 3D profiles of the machined surface obtained by an optical interferometric profiler, the measured groove depths, and surface roughness of machined area. Clearly, the solution temperature influences the machining efficiency. The greater the temperature difference between the solution and the environment, the higher the efficiency of the jet machining, due to the faster crystal precipitation rate caused by a larger temperature difference.

Compared to temperature, the nature of the salt appears to have a more significant impact. As mentioned earlier, $NaH_2PO_4$ possesses the steepest solubility/temperature slope, yet paradoxically exhibits lower machining efficiency than $NaNO_3$. The machined depth of $NaH_2PO_4$ was approximately only half of that by $NaNO_3$. And another interesting phenomenon was that $CaCl_2$ has a solubility/temperature slope similar to that of $NaNO_3$, or even steeper in the temperature range from 20 to 40 °C, it produced no discernible machining effect under any of the three temperature conditions.

Regarding the surface roughness of machined areas, as shown in Fig. 3c, most values of Ra were below 2 μm, with the exception of $NaNO_3$ of 50 °C. Typically, higher jet machining efficiency correlates with increased surface roughness. This trend is also shown in Fig. 3. As the temperature increased from 30 °C to 40 °C and 50 °C, both machining depth and surface roughness increased correspondingly.

However, comparing the results by $NaNO_3$ and $NaH_2PO_4$, it is interesting that at the same temperature, despite their significantly different machining efficiencies, their surface roughness values were relatively close, particularly at 30 °C and 40 °C. Understanding this phenomenon likely requires systematic investigation into the synergy effects of morphology and size distribution of crystals formed during

**Table 1**
Experimental parameters.

| Operating parameter | Range |
|---|---|
| Nozzle outlet diameter | 2.8 mm |
| Air pressure | 0.5 MPa |
| Jet angle | 90 ° |
| Jet distance | 5 mm |
| Ambient temperature | 20 DC |
| Mask opening | 1000 μm |
| Mask thickness | 0.1 mm |
| Feed speed | 0.2 mm/s |
| Feed pitch | 1 mm |

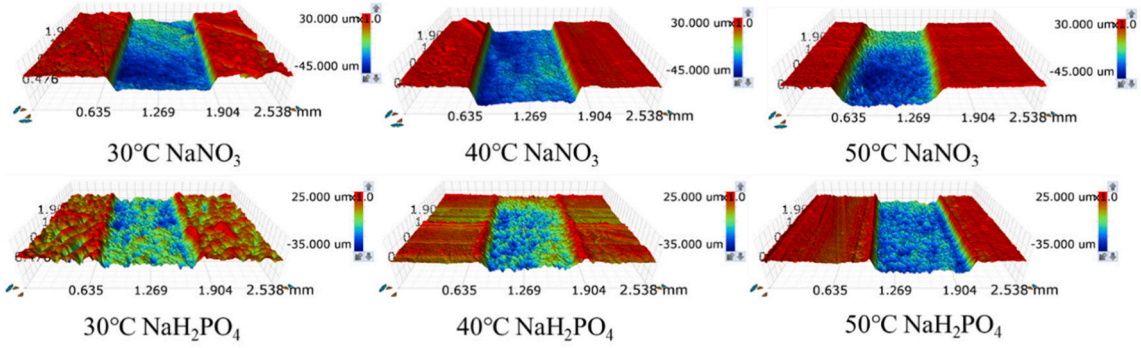


(a) Profiles of machined surface

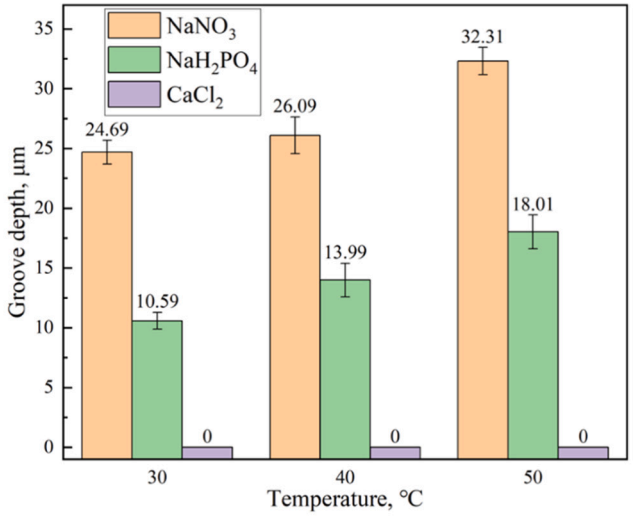


(b) Groove depth

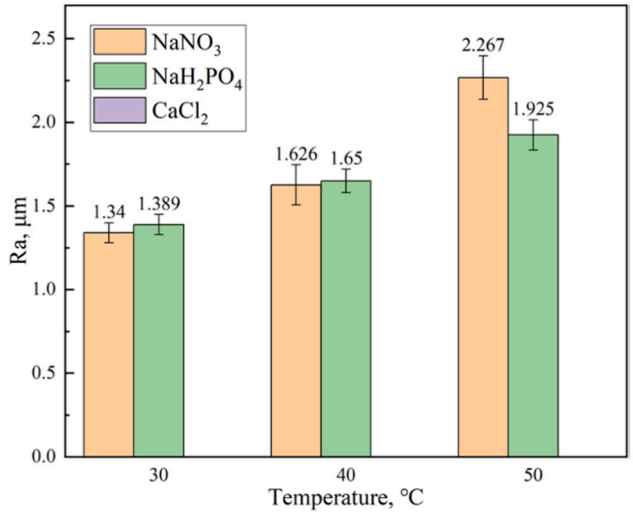


(c) Surface roughness of machined area

**Fig. 3.** Machining capacity using selected salt-saturated solutions at different solution temperatures.
(a) Profiles of machined surface.
(b) Groove depth.
(c) Surface roughness of machined area.

their precipitation processes.

In order to understand the differences in machining effectiveness among the various salt solutions, attempts were made to observe the particle morphologies crystallizing during the jetting process. The left column of Fig. 4 shows images captured using a high-speed camera, in which crystalline particles appear to be forming within the jet stream. The middle column of Fig. 4 displays the corresponding crystalline particles collected after jetting, demonstrating that crystalline particles are indeed generated during the jetting process.

However, it is difficult to obtain clear, direct images of the morphology of crystals coexisting with water. This is because the water adhering to the crystal surfaces is hard to remove, and the salts used all have high solubility; thus, collected crystals immediately begin dissolving upon temperature change. As shown in Fig. 4 a3 and b3, it can be discerned that $NaNO_3$ crystals exhibit a hexahedral shape, while $NaH_2PO_4$ crystals form multi-faceted pyramidal structures. For $CaCl_2$, observing its crystal morphology directly was exceedingly difficult. Consequently, Fig. 4c3, the image depicting $CaCl_2$ morphology was sourced from reference material, not captured in this study. It shows that $CaCl_2$ crystallizes into a filament-like morphology. Although the crystals formed within the jet would not be this long, it is evident that this form is not good abrasives. It appears that the hexahedral crystalline particles formed by $NaNO_3$ provide better machining effectiveness than the pyramidal crystals of $NaH_2PO_4$. This difference in crystal morphology partially explains the variations in machining depth observed in Fig. 3.

Fig. 5 shows a spiral groove machined on a PTFE composite sealing ring using a saturated $NaNO_3$ solution. The machined profile is clear and smooth, the machined bottom surface is flat, and the depth and dimensions meet the requirements of surface texture design. It validates the feasibility of using SGAJM jet machining for surface texturing, effectively resolving the issue of residual hard abrasives encountered during the machining of soft materials.

The SGAJM jet machining approach is just proposed. To gain a deeper understanding of its machining mechanisms and optimize its process, there should be many issues need to be studied, such as the hardness of the abrasive particles, the influence of the precipitation process on machining, and the range of machinable materials.

## 5. Conclusions

To solve the problem of residual hard abrasives in jet machining processes, this study proposes a self-generating abrasive jet machining (SGAJM) approach. By preliminary experimental verification, the conclusions can be drawn as follows.

1) The feasibility of the proposed SGAJM jet machining approach has been confirmed by experiments. By utilizing highly soluble salts as abrasives, residues can be removed through simple rinsing, effectively resolving the problem of residual hard abrasives.
2) This method employs compressed air accelerated through a nozzle to generate a pressure drop and low temperatures, which draws in a saturated solution and precipitates crystalline abrasives, thereby forming a multiphase jet. The approach is simple and practical.
3) For the salts used in SGAJM jet machining, not only must they possess a favorable solubility/temperature slope, but their crystallization kinetics and resulting crystal morphology are also critical factors influencing machining effectiveness.
4) Through preliminary optimization, SGAJM jet machining successfully produced surface textures on PTFE composite materials.

## CRediT authorship contribution statement

**Yan Hu:** Writing – original draft, Methodology, Funding acquisition, Conceptualization. **Jianchi Chen:** Visualization, Investigation, Formal analysis. **Qingwen Dai:** Validation, Methodology. **Wei Huang:** Resources, Data curation. **Jingqiu Wang:** Visualization, Validation. **Xiaolei Wang:** Writing – review & editing, Supervision, Funding acquisition, Conceptualization.

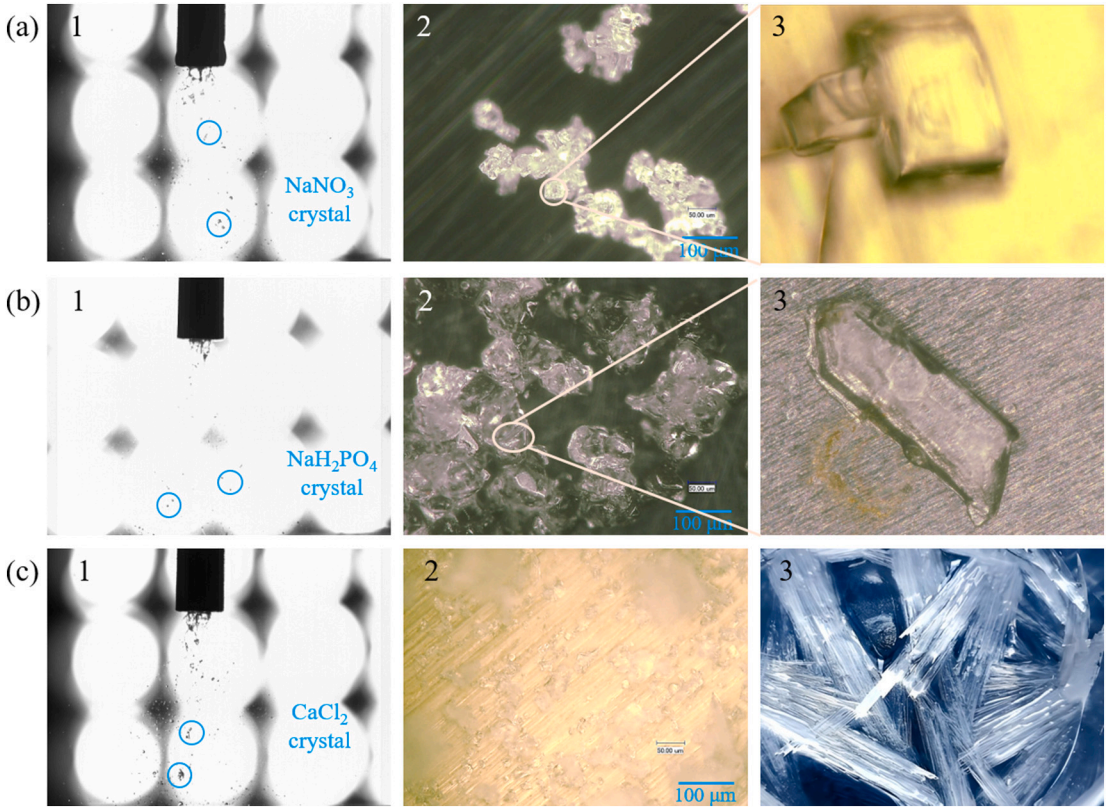


**Fig. 4.** The morphology of precipitated crystals: (a) $NaNO_3$, (b)$NaH_2PO_4$, (c)$CaCl_2$.

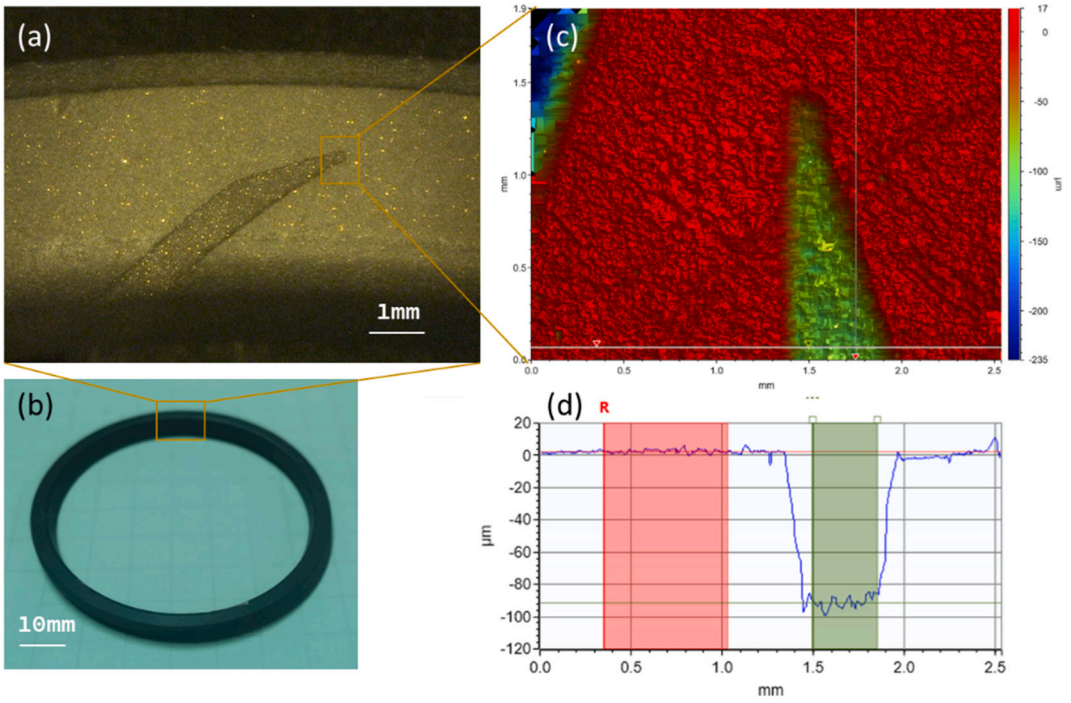


**Fig. 5.** Groove fabricated on the mechanical seal made of PTFE composite: (a) Optical image of machined groove, (b) PTFE composite seal, (c) Groove profile by interferometric profiler, (d) Section profile.

## Declaration of competing interest

The authors declare the following financial interests/personal relationships which may be considered as potential competing interests: Xiaolei WANG reports financial support was provided by National Natural Science Foundation of China. Yan HU reports financial support was provided by National Natural Science Foundation of China. If there are other authors, they declare that they have no known competing financial interests or personal relationships that could have appeared to influence the work reported in this paper.

## Acknowledgments

The authors are grateful for the support provided by the National Natural Science Foundation of China (52175172, 52405445).

## References

[1] Gachot C, Rosenkranz A, Hsu SM, Costa HL. A critical assessment of surface texturing for friction and Wear improvement. Wear 2017;372-373:21–41.
[2] Yu H, Huang W, Wang X. Dimple patterns Design for Different Circumstances. Lubr Sci 2013;25:67–78.
[3] Melentiev R, Fang F. Recent advances and challenges of abrasive jet machining. CIRP J Manuf Sci Technol 2018;22:1–20.
[4] Nouraei H, Wodoslawsky A, Papini M, Spelt JK. Characteristics of abrasive slurry jet Micro-machining: a comparison with abrasive air jet Micro-machining. J Mater Process Technol 2013;213(10):1711–24.
[5] Wang J, Jing Y, Du X, Zheng L, Wang C, Chen P. Abrasive water machining - state of the art and future perspectives. J Mech Eng 2024;60:1–32.
[6] Zhang G, Ma W, Gao Y, Zhao Y, Zhao G, Meng J, et al. Clarification of the effect of cooling rate on abrasive embedding behavior of Pdms in cryogenic abrasive air-jet machining. J Manuf Process 2025;134:749–61.
[7] Liao Z, Sanchez I, Xu D, Axinte D, Augustinavicius G, Wretland A. Dual-processing by abrasive waterjet machining—a method for machining and surface modification of nickel-based Superalloy. J Mater Process Technol 2020;285:116768.
[8] Gradeen AG, Spelt JK, Papini M. Cryogenic abrasive jet machining of polydimethylsiloxane at different temperatures. Wear 2012;274-275:335–44.
[9] Zhao Y, Zhao X, Chen X, Song J, Cui Y, Niu F, et al. Modeling and analysis of plastic abrasive jet flow characteristics. J Manuf Process 2024;123:96–111.
[10] Chai T, Huang C, Li H, Cheng H, Wu Z, Long X. Research on influencing factors of degradable soft abrasive water jet on remanufacturing cleaning performance. J Hunan Univ 2024;51(4):71–81.
[11] Zhu Y, Wu J, Lu W, Zuo D, Xiao H, Cao D, et al. Surface formation mechanics and its microstructural characteristics of Aajp of aluminum alloy by using amino thermosetting plastic abrasive. Int J Precis Eng Manuf-Green Technol 2020;9(1):59–72.
[12] Uhlmann E, Kretzschmar M, Elbing F, Mihotovic V. Deburring with Co2 snow blasting. In: Proceedings on the CIRP, international conference on burrs. Springer: University of Kaiserslautern; 2009. p. 181–7.
[13] Karpuschewski B, Petzel M. Ice blasting – An innovative concept for the problem-oriented deburring of workpieces. In: Proceedings on the CIRP, international conference on burrs. Germany: University of Kaiserslautern; 2009. p. 197–201.
[14] Guo P, Zhao W, Hao Y, Yang T. Influence factors of soluble crystal properties on cutting quality of biological bone materials. Diamond Abras Eng 2023;43:144–50.
[15] Thomas PJ. Simulation of industrial processes for control engineers. Oxford: Butterworth-Heinemann; 1999.
[16] Momber A. Blast Cleaning Technology. Berlin: Springer-Verlag Berlin Heidelberg; 2008.
[17] Hu Y, Dai Q, Huang W, Wang X. Characteristics of multiphase jet machining: a comparison with the absence of water. J Mater Process Technol 2021;291:117050.